

Supporting Information for

Dual-Emissive Monoruthenium Complexes of N(CH₃)-Bridged
Ligand: Synthesis, Characterization, and Substituent Effect

*Si-Hai Wu, *† Zhe Zhang, † Ren-Hui Zheng, † Rong Yang, † Lianhui Wang, *‡
Jiang-Yang Shao, ‡ Zhong-Liang Gong, *‡ and Yu-Wu Zhong†*

† School of Medicine, Huaqiao University, Quanzhou, Fujian 362021, China

‡ CAS Key Laboratory of Photochemistry, CAS Research/Education Center for Excellence in Molecular Sciences, Institute of Chemistry, Chinese Academy of Sciences, Beijing 100190, China

*To whom correspondence should be addressed. Email: wusihai@hqu.edu.cn; lianhui.wang@hqu.edu.cn; gongzhongliang@iccas.ac.cn

Table of Contents

NMR spectra of L1 , L3 , 1(PF₆)₂ , and 3(PF₆)₂	S2–S5
Mass spectra of 1(PF₆)₂ , 2(PF₆)₂ , and 3(PF₆)₂	S6
HPLC spectra of complexes 1(PF₆)₂–3(PF₆)₂	S7
Single-Crystal X-Ray data of complex 3(PF₆)₂	S7
Photophysical studies of these compounds	S8–S10
Electrochemical data of ligands L1–L3	S10
DFT/TD-DFT calculation results of these complexes	S11–S12

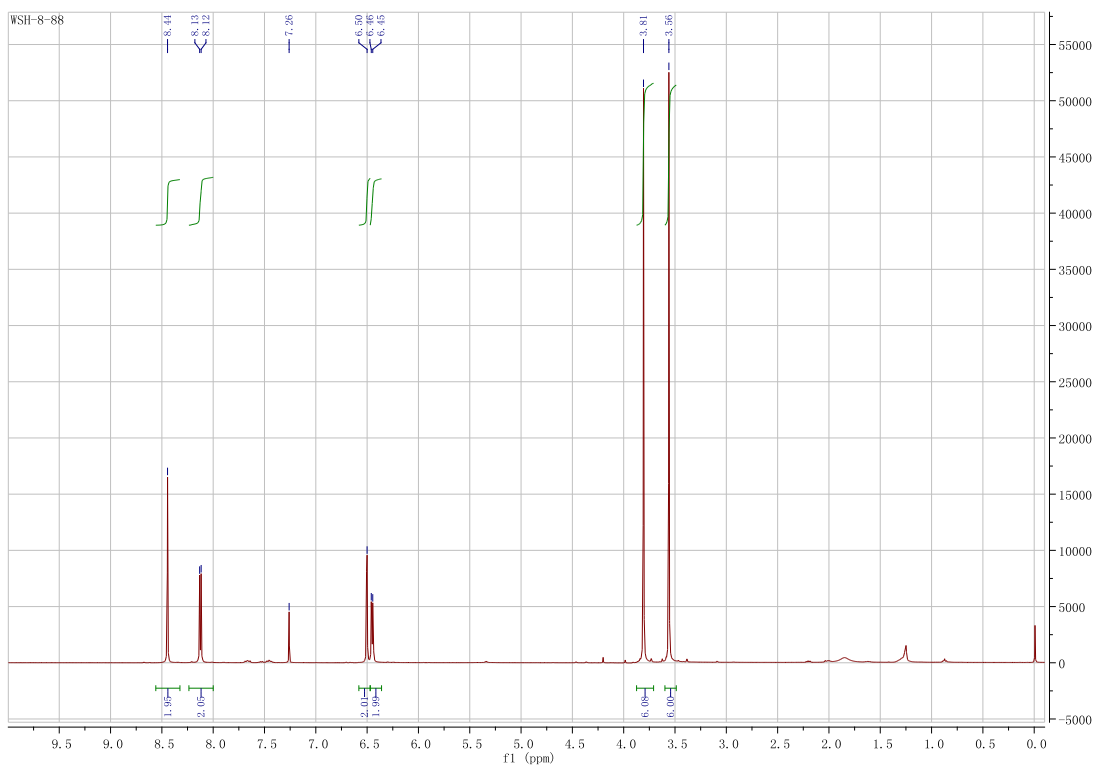


Figure S1. ^1H NMR spectra of **L1** in CDCl_3 .

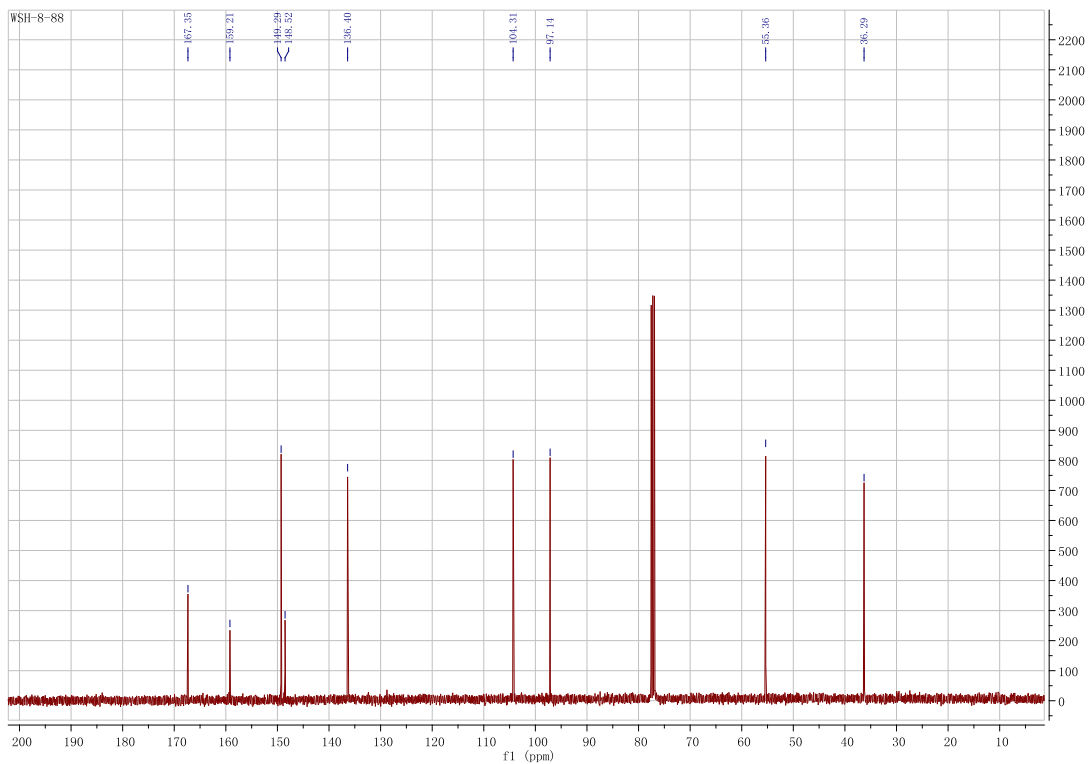


Figure S2. ^{13}C NMR spectra of **L1** in CDCl_3 .

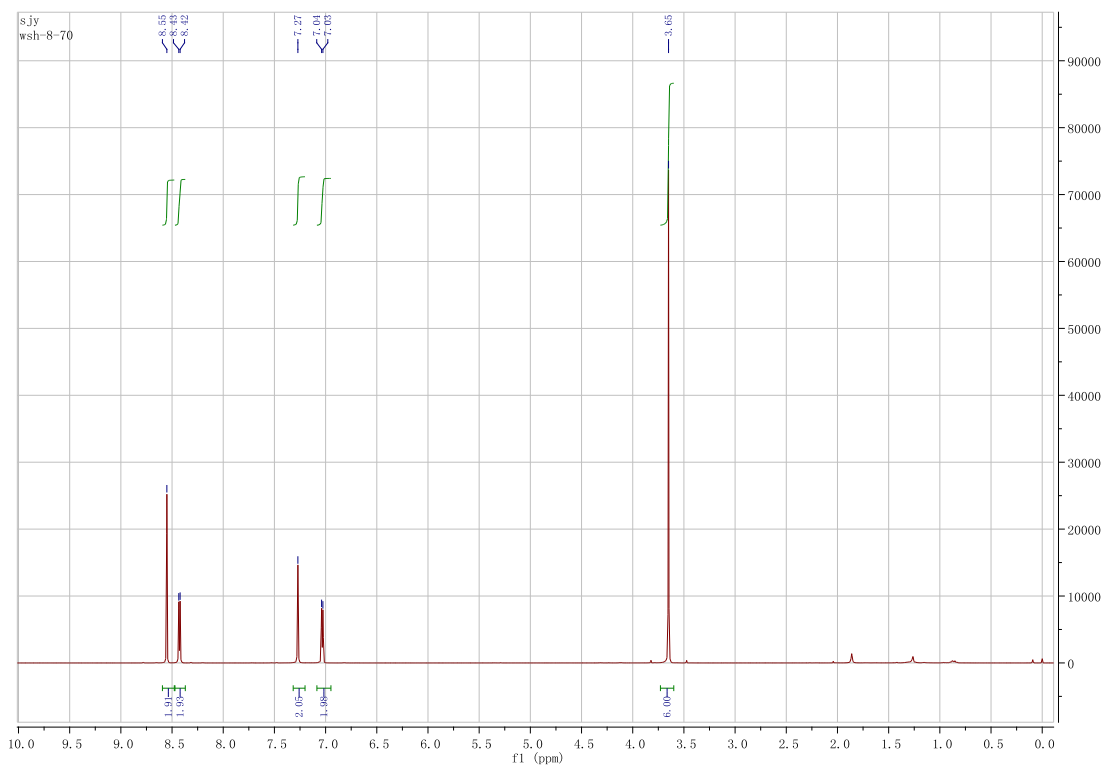


Figure S3. ¹H NMR spectra of **L3** in CDCl_3 .

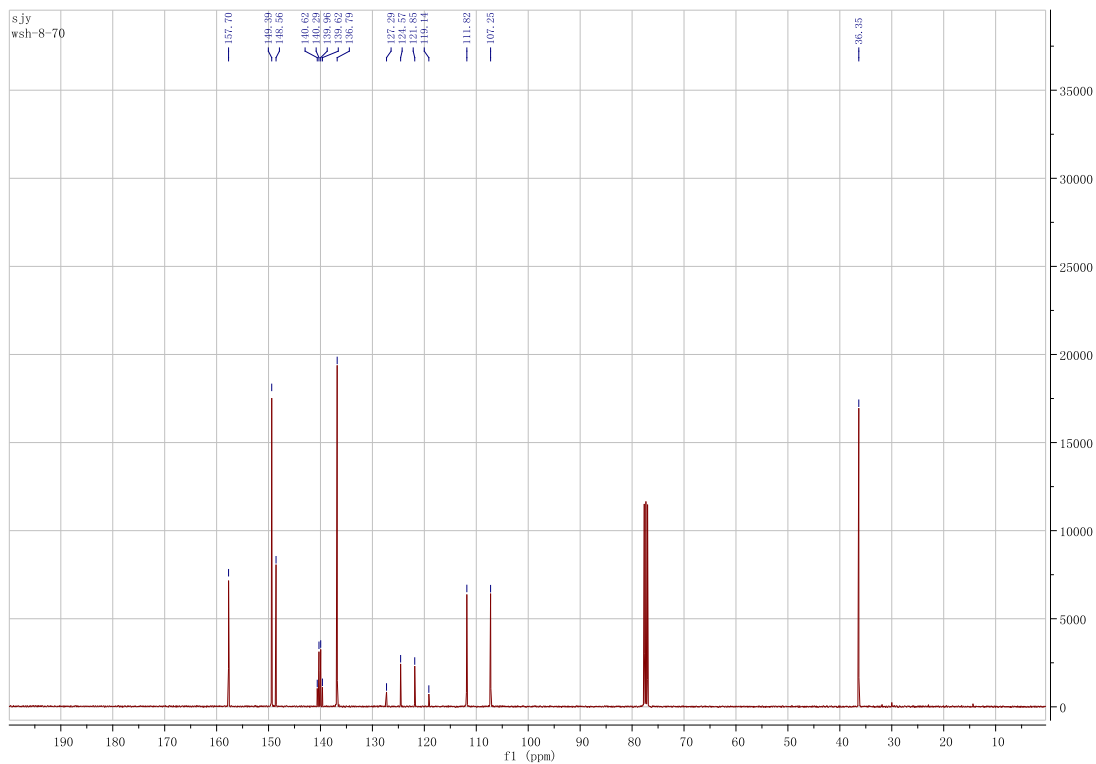


Figure S4. ¹³C NMR spectra of **L3** in CDCl_3 .

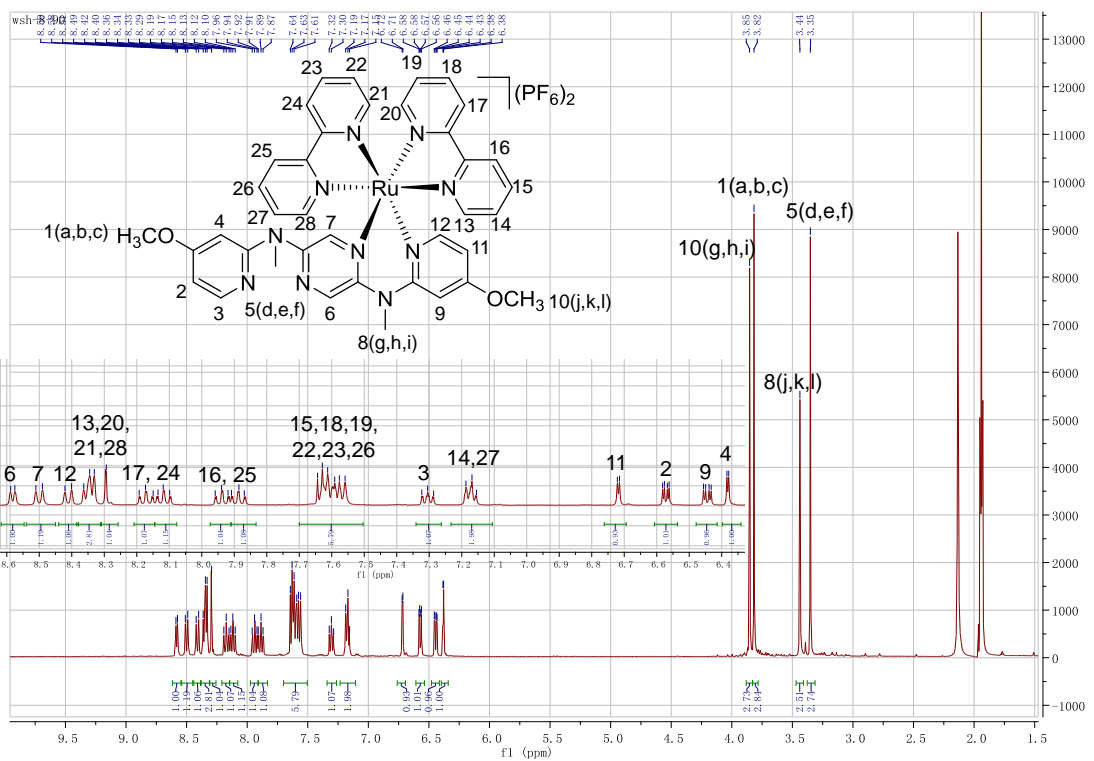


Figure S5. ¹H NMR spectra of **1**(PF_6)₂ in CD_3CN .

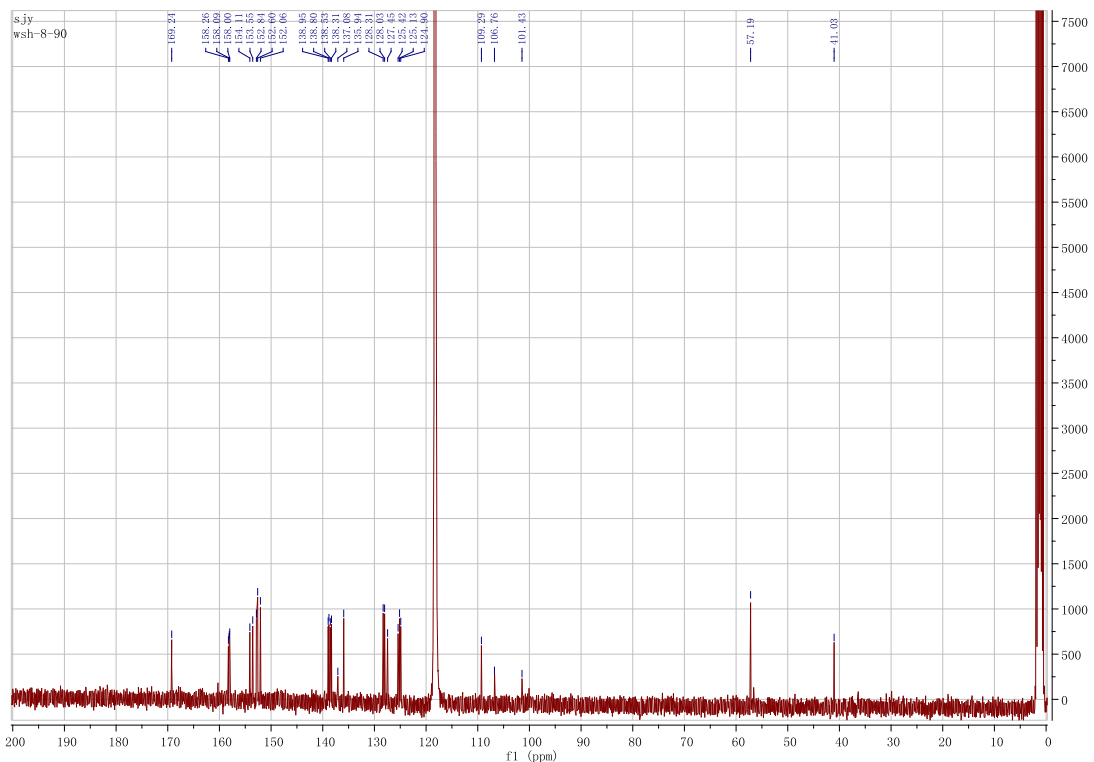


Figure S6. ¹³C NMR spectra of **1**(PF_6)₂ in CD_3CN .

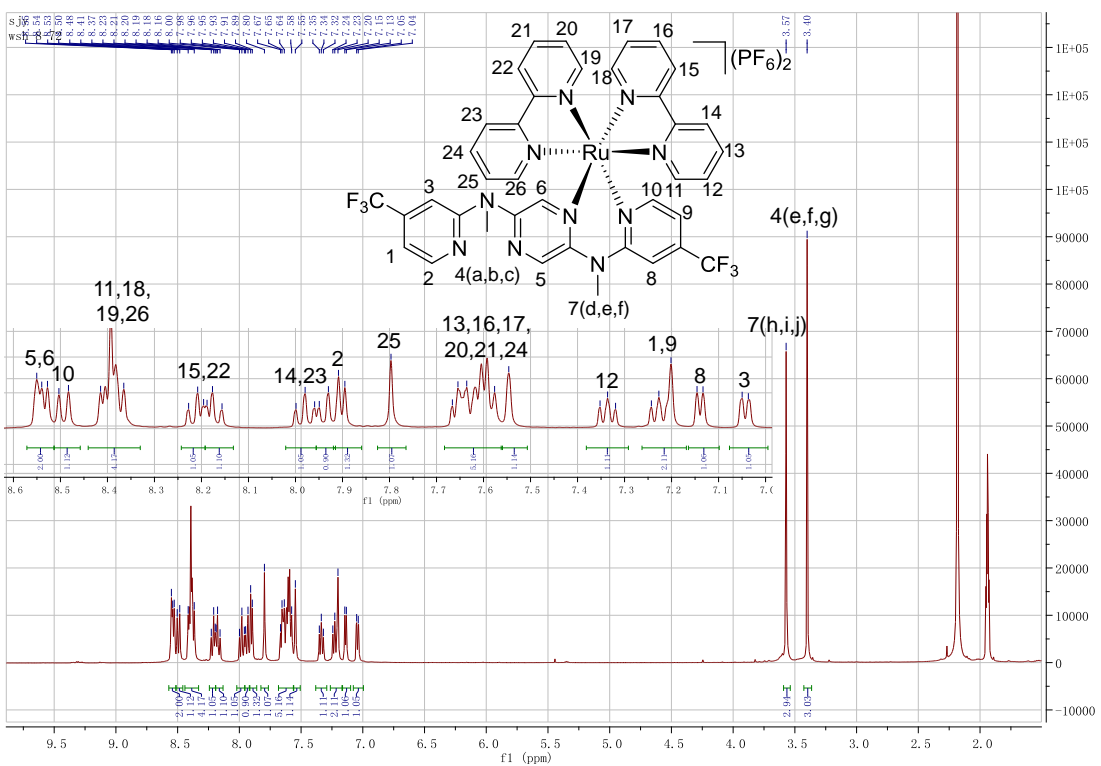


Figure S7. ¹H NMR spectra of **3**(PF₆)₂ in CD₃CN.

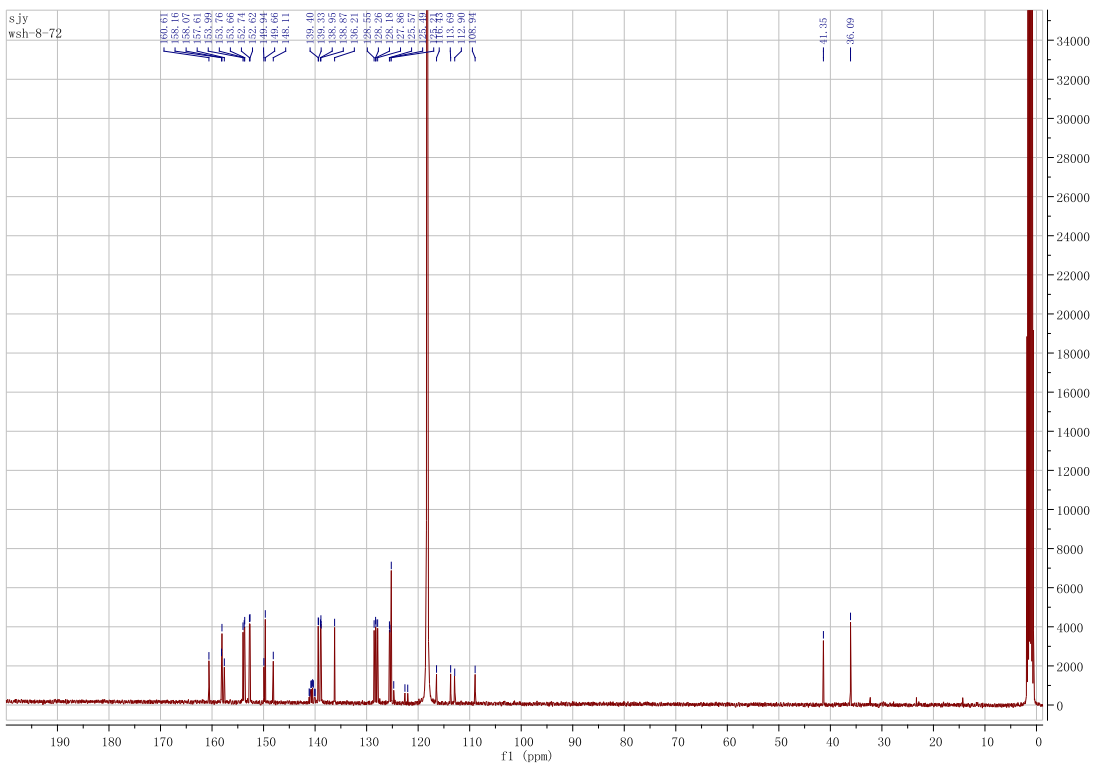


Figure S8. ¹³C NMR spectra of **3**(PF₆)₂ in CD₃CN.

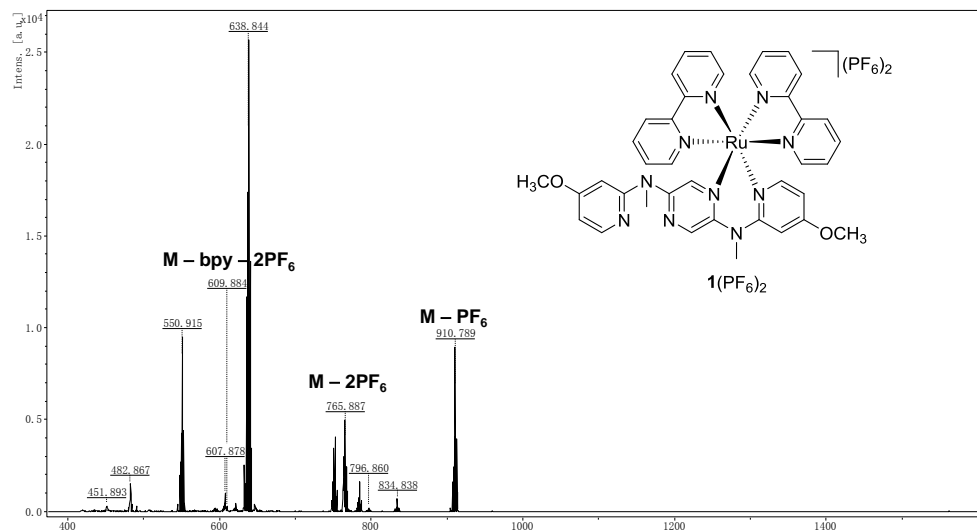


Figure S9. MADLI-TOF mass spectrum of $\mathbf{1}(\text{PF}_6)_2$.

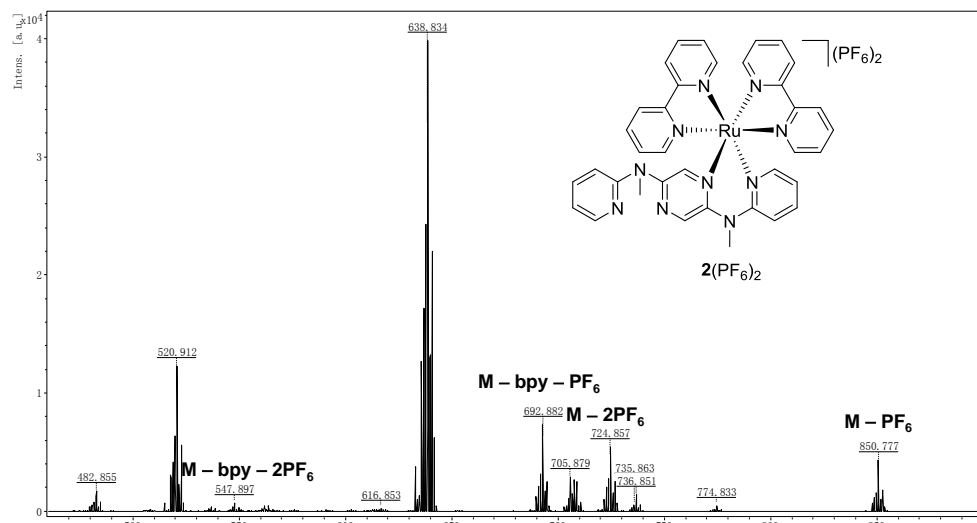


Figure S10. MADLI-TOF mass spectrum of $\mathbf{2}(\text{PF}_6)_2$.

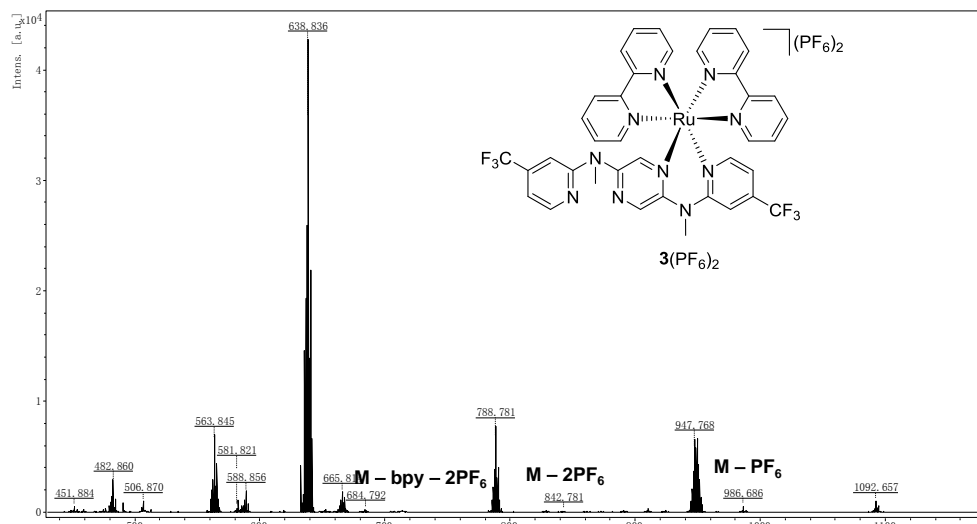


Figure S11. MADLI-TOF mass spectrum of $\mathbf{3}(\text{PF}_6)_2$.

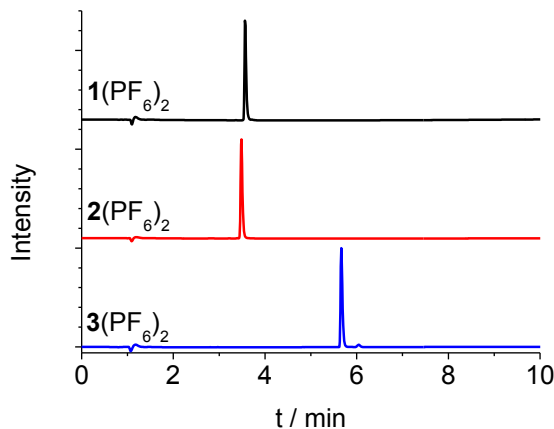


Figure S12. Analytical HPLC spectra of **1**(PF₆)₂ (black line), **2**(PF₆)₂ (red line), and **3**(PF₆)₂ (blue line). The noise peaks around 1.1 s are due to eluent solvents.

Table S1. Single-crystal X-ray data of complex **3**(PF₆)₂.

Compound	3 (PF ₆) ₂
CCDC number	2107266
Empirical formula	C ₃₈ H ₃₀ F ₁₈ N ₁₀ P ₂ Ru
Formula mass	1131.73
Crystal system	Triclinic
<i>a</i> [Å]	11.6715(4)
<i>b</i> [Å]	13.8183(4)
<i>c</i> [Å]	14.1803(4)
<i>V</i> [Å ³]	2107.13(12)
α [°]	74.878(3)
β [°]	74.737(3)
γ [°]	78.194(2)
<i>Z</i>	2
Density [Mg·cm ⁻³]	1.784
<i>R</i> 1 (final)	0.0477
<i>wR</i> 2 (final)	0.1105
<i>R</i> 1 (all)	0.0585
<i>wR</i> 2 (all)	0.1155

Table S2. Selected bond lengths (Å) and angles.

Complex	Bond lengths (Å)	Bond angles	
3 (PF ₆) ₂	Ru(1)–N(1)	2.056(3)	N(1)–Ru(1)–N(6) 78.86(11)
	Ru(1)–N(2)	2.078(3)	N(2)–Ru(1)–N(3) 78.68(11)
	Ru(1)–N(3)	2.062(3)	N(4)–Ru(1)–N(5) 88.30(10)
	Ru(1)–N(4)	2.068(3)	N(2)–Ru(1)–N(4) 91.11(10)
	Ru(1)–N(5)	2.099(3)	N(2)–Ru(1)–N(5) 97.14(10)
	Ru(1)–N(6)	2.071(3)	N(1)–Ru(1)–N(2) 96.38(11)

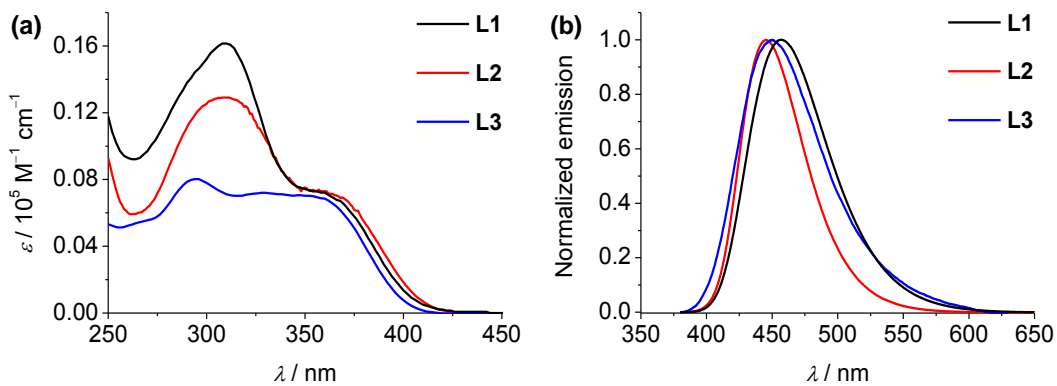


Figure S13. (a) UV-vis absorption spectra of ligand **L1–L3** in acetonitrile. (b) Emission spectra of ligand **L1–L3** in acetonitrile on excitation at 360 nm.

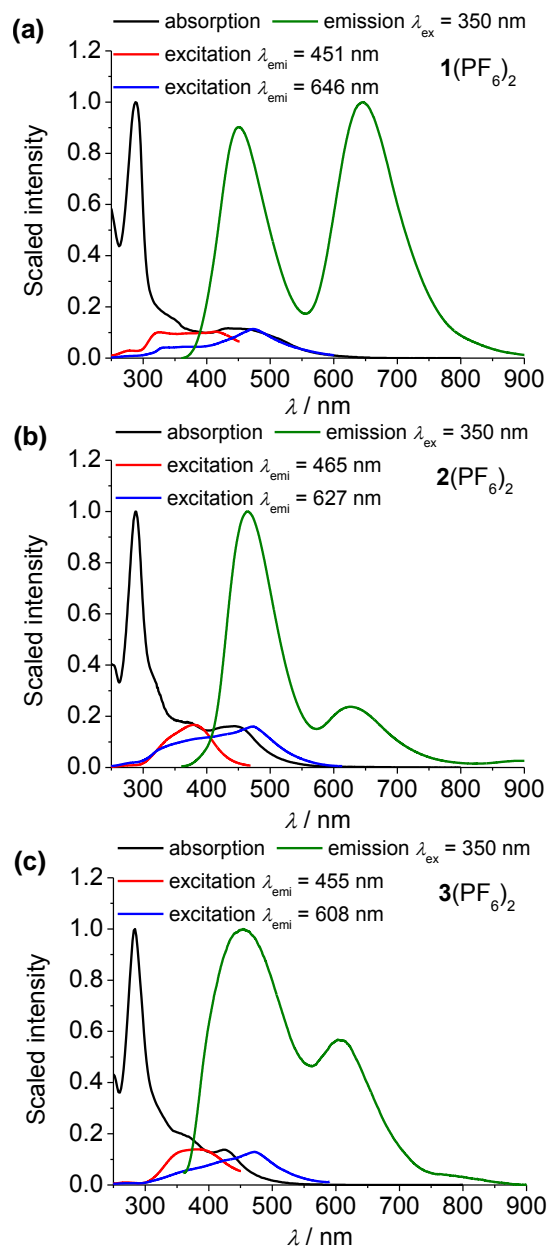


Figure S14. Absorption, excitation, and emission spectra of **1**(PF_6)₂ (a), **2**(PF_6)₂ (b), and **3**(PF_6)₂ (c) in CH_3CN .

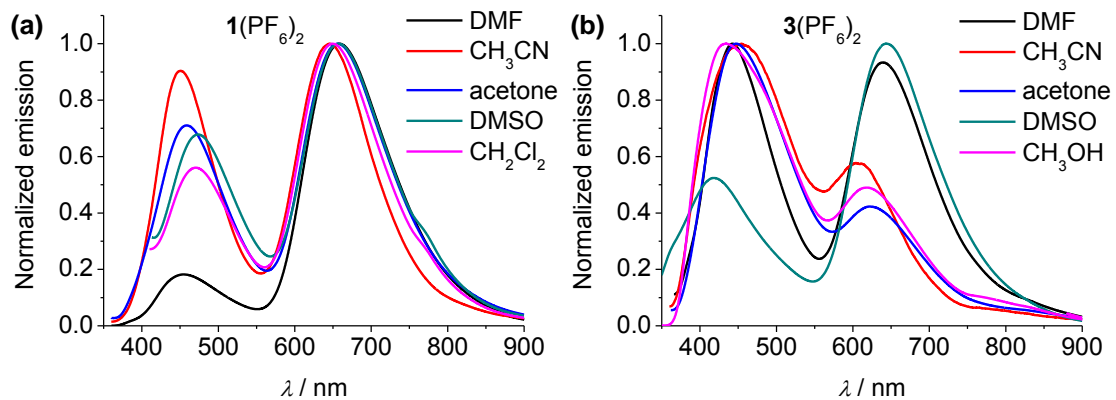


Figure S15. Normalized emission spectra changes of $\mathbf{1}(\text{PF}_6)_2$ (a) and $\mathbf{3}(\text{PF}_6)_2$ (b) in different solvents.

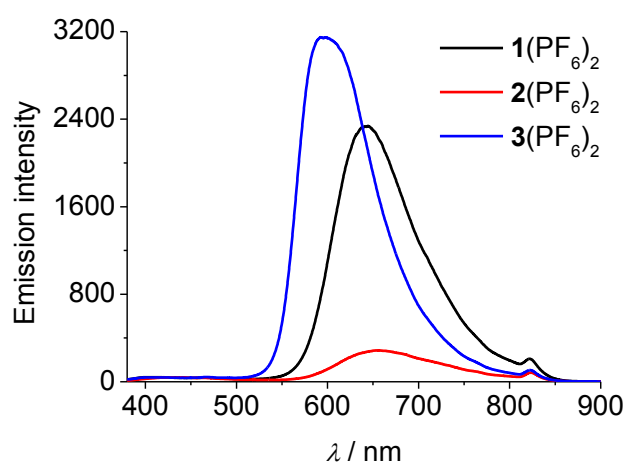


Figure S16. Emission spectra of $\mathbf{1}(\text{PF}_6)_2$ (a), $\mathbf{2}(\text{PF}_6)_2$ (b), and $\mathbf{3}(\text{PF}_6)_2$ (c) in solid state on excitation at 350 nm.

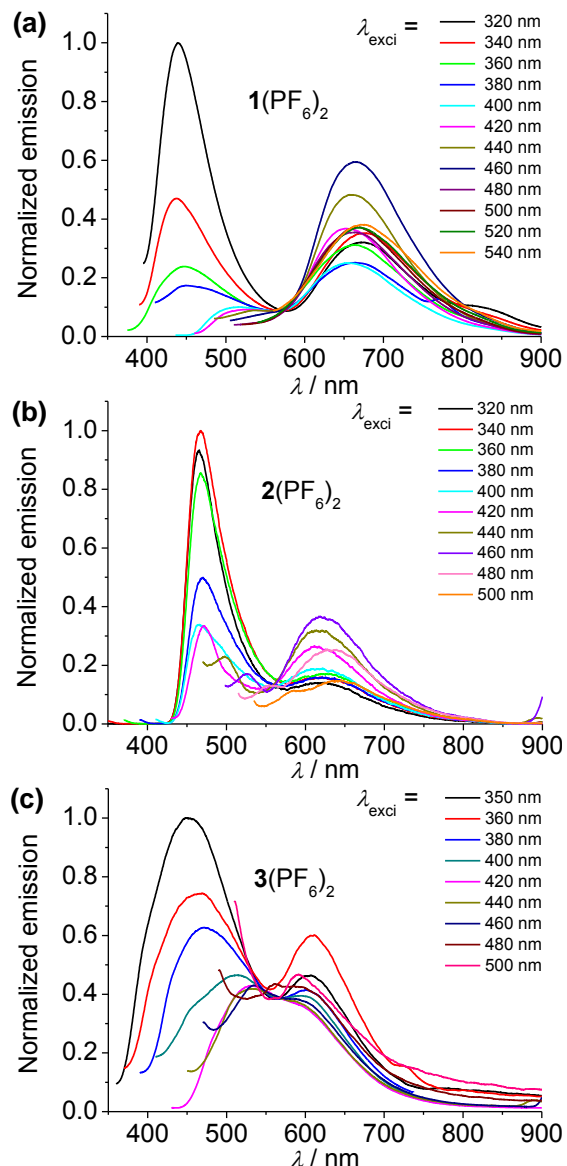


Figure S17. Emission spectra changes of $\mathbf{1}(\text{PF}_6)_2$ (a), $\mathbf{2}(\text{PF}_6)_2$ (b), and $\mathbf{3}(\text{PF}_6)_2$ (c) in CH_3CN at different excitation wavelength.

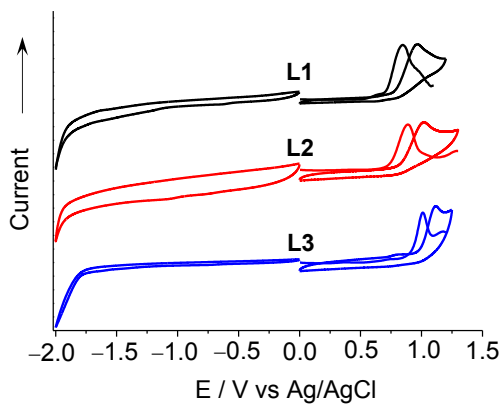


Figure S18. CVs and DPVs of ligands **L1–L3** in acetonitrile containing 0.1 M Bu_4NClO_4 at a scan rate of 100 mV/s. The working electrode is a glassy carbon, the counter electrode is a Pt wire, and the reference electrode is Ag/AgCl in saturated aq. NaCl.

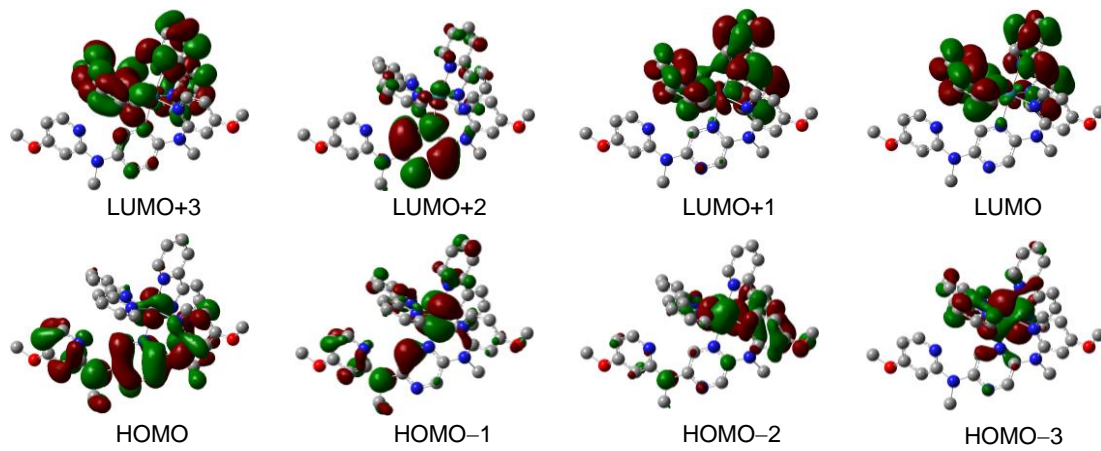


Figure S19. Isodensity plots of selected frontier molecular orbitals of complex $\mathbf{1}^{2+}$. All orbitals were computed at an isovalue of 0.02 e bohr^{-3} .

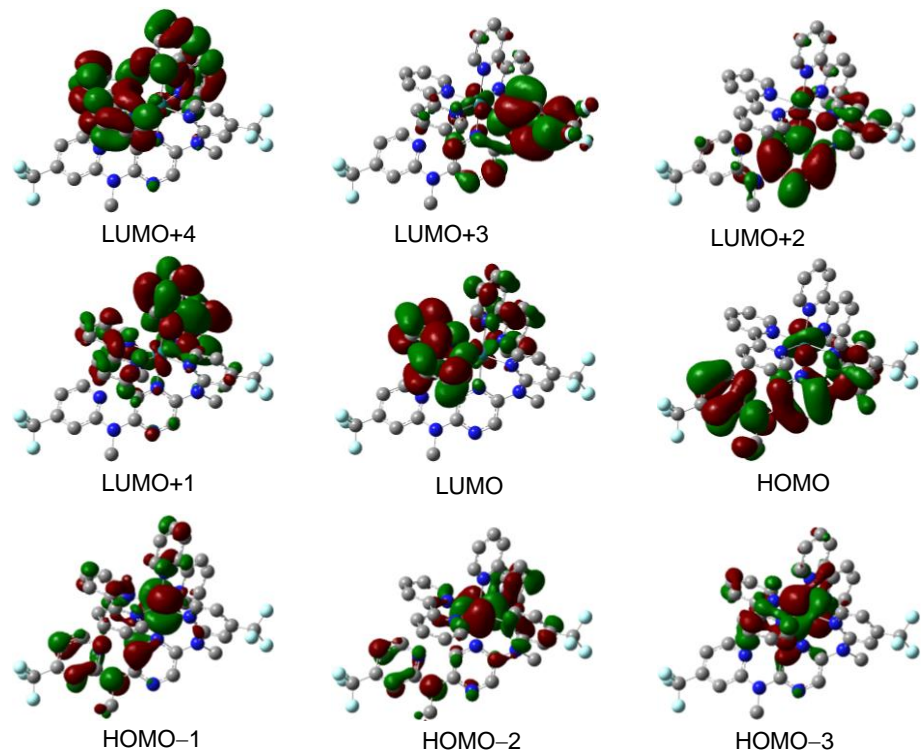


Figure S20. Isodensity plots of selected frontier molecular orbitals of complex $\mathbf{3}^{2+}$. All orbitals were computed at an isovalue of 0.02 e bohr^{-3} .

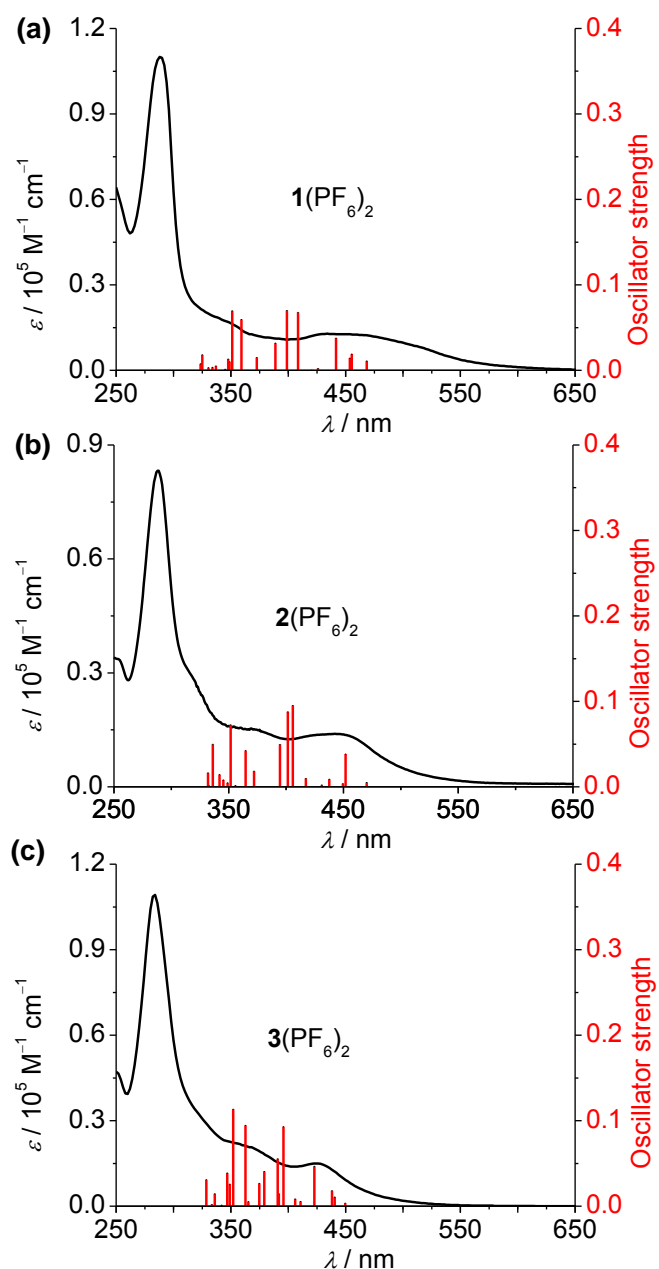


Figure S21. TDDFT-predicted excitations (red lines) of (a) **1**²⁺, (b) **2**²⁺, and (c) **3**²⁺. The absorption spectra of **1(PF₆)₂**–**3(PF₆)₂** (black curves) are included for comparison.